THE JOURNAL OF BIOLOGICAL CHEMISTRY VOL. 283, NO. 32, pp. 22304–22315, August 8, 2008

G2E3 Is a Dual Function Ubiquitin Ligase Required for Early Embryonic Development*

Received for publication, April 28, 2008, and in revised form, May 23, 2008 Published, JBC Papers in Press, May 28, 2008, DOI 10.1074/jbc.M803238200

William S. Brooks[‡1], E. Scott Helton[‡], Sami Banerjee[§], Melanie Venable[¶], Larry Johnson[‖], Trenton R. Schoeb[‖], Robert A. Kesterson[‖], and David F. Crawford[‡§2]

From the Departments of [‡]Cell Biology, [‖]Genetics, [§]Pediatrics, and [¶]School of Medicine, University of Alabama, Birmingham, Alabama 35233

G2E3 is a putative ubiquitin ligase (E3) identified in a microarray screen for mitotic regulatory proteins. It shuttles between the cytoplasm and nucleus, concentrating in nucleoli and relocalizing to the nucleoplasm in response to DNA damage. In this study, we demonstrate that G2E3 is an unusual ubiquitin ligase that is essential in early embryonic development to prevent apopotic death. This protein has a catalytically inactive HECT domain and two distinct RING-like ubiquitin ligase domains that catalyze lysine 48-linked polyubiquitination. To address *in vivo* function, we generated a knock-out mouse model of G2E3 deficiency that incorporates a β-galactosidase reporter gene under control of the endogenous promoter. Animals heterozygous for G2E3 inactivation are phenotypically normal with no overt change in development, growth, longevity, or fertility, whereas *G2E3* null embryos die prior to implantation. Although normal numbers of *G2E3*$^{-/-}$ blastocysts are present at embryonic day 3.5, these blastocysts involute in culture as a result of massive apoptosis. Using β-galactosidase staining as a marker for protein expression, we demonstrate that G2E3 is predominantly expressed within the central nervous system and the early stages of limb bud formation of the developing embryo. In adult animals, the most intense staining is found in Purkinje cell bodies and cells lining the ductus deferens. In summary, G2E3 is a dual function ubiquitin ligase essential for prevention of apoptosis in early embryogenesis.

The sequence and timing of events in the cell division cycle are highly regulated to prevent aneuploidy and the development of malignancies (1, 2), as well as to ensure normal embryonic development (3). Similarly, proteins that regulate the response to and repair of damaged DNA are also essential in maintenance of genomic integrity and normal development. Although many proteins involved in cell cycle regulation and DNA damage signaling are known, we and others have conducted studies to identify other molecules involved in these processes (4–7). In our study, we identified about 50 genes that were expressed in a G_2/M-specific manner, many of which were down-regulated in response to DNA damage. Many of these genes have been shown to play a role in important cell cycle events or checkpoints including cyclin B1 (8), Plk1 (9), Tome-1 (10), Aurora-A (11), Ube2Q2 (12), topoisomerase IIα, CENP-A (13), Nuf-2R (14), and others. Because protein ubiquitination plays an essential role in many aspects of cell cycle regulation and checkpoint function, it is not surprising that many of the genes identified in our study are thought to function in this process. Included among these are an APC/C component (Cdc20) (15, 16), an SCF component (Tome-1) (10), the ubiquitin conjugating enzymes E2-EPF (17, 18), and UBE2Q2 (12), and a putative ubiquitin ligase known as G2E3 (19).

G2E3 displays dynamic subcellular localization, concentrating within nucleoli but relocalizing to the nucleoplasm after genotoxic stress (19). These data suggest a possible role for G2E3 in regulation of mitosis and the response to DNA damage. G2E3 has a C-terminal HECT (homologous to E6-associated protein C terminus) domain, a motif that typically functions in ubiquitination. In addition, there are three N-terminal zinc finger domains with varying similarity to both RING (Really Interesting New Gene) and PHD (plant homeodomain) domains. Many RING domains function as ubiquitin ligase catalytic domains (20), and an increasing number of PHD domains have this activity (21–25), although some controversy remains about the appropriate designation of such domains as either RING or PHD domains (26, 27). Until recently, all known ubiquitin ligases had a single E3 catalytic domain, but Msc1, an *Schizosaccharomyces pombe* protein involved in checkpoint function, was recently shown to have three ubiquitin ligase domains (22).

Embryonic development is dependent on the coordinated division of cells in the embryo that must be performed without introduction of mutations in the genetic material. Therefore, it is not surprising that molecules that regulate cell division and checkpoint responses are among the most important proteins in embryonic development. For example, inactivation of one or more *Cyclin* or *Cdk* genes has been associated with a variety of specific developmental abnormalities such as splenic and thymic hypoplasia, cardiac anomalies, hematopoietic defects, neuropathy, sterility, and death (reviewed in Ref. 28). Embryonic lethality is associated with disruption of other single cell cycle

* This work was supported, in whole or in part, by National Institutes of Health Grants P30 CA13148 (to the University of Alabama Comprehensive Cancer Center Core), P30 AR48311 (to the Rheumatic Diseases Core Center) and K08CA86941. This work was also supported grants from the Hope Street Kids Foundation and The Research Institute at Children's Hospital (Children's Hospital of Alabama (DFC)). The costs of publication of this article were defrayed in part by the payment of page charges. This article must therefore be hereby marked "*advertisement*" in accordance with 18 U.S.C. Section 1734 solely to indicate this fact.

[1] Present address: Dept. of Biology, Freed-Hardeman University, Henderson, TN 38340.

[2] To whom correspondence should be addressed: 940 Stanton L. Young Blvd., BMSB 311, Oklahoma University Health Science Center, Oklahoma City, OK 73104. Tel.: 405-271-8001, ext. 52655; Fax: 405-271-3756; E-mail: david-crawford@ouhsc.edu.

regulatory genes including *Emi1* (29), *Cdk11* (30), and *Cyclins B1* (31) and *A2* (32). Many proteins that regulate cell cycle checkpoints are also important in embryonic development. For example, mutations in both *ATM* and *FANC* proteins cause an array of developmental abnormalities in individuals with ataxia telangiectasia (33) and Fanconi anemia (34), as well as mice harboring disruptions of the murine orthologs (35, 36). The importance of DNA damage responses in embryonic development is further emphasized by the embryonic lethality resulting from disruption of *Atr*, *Chk1*, *Brca1* (an ubiquitin ligase), *Brca2*, and *Rad51* (37–42).

In this study, we have characterized the biochemical activity of G2E3, demonstrating that it functions as an ubiquitin ligase using two distinct catalytic domains. Furthermore, we have generated *G2E3* knock-out mice and shown that the protein is essential in early embryonic development for prevention of massive apoptosis leading to involution of blastocysts. Finally, using β-galactosidase activity as a marker for expression of *G2E3*, we showed that this gene is expressed in the developing central nervous system and at lower levels at several other anatomic locations. In summary, G2E3 is a dual function ubiquitin ligase that performs an essential role in early embryonic development by blocking apoptosis.

EXPERIMENTAL PROCEDURES

Preparation of Recombinant G2E3 and E6-AP—Cysteine to alanine mutations of *G2E3* were generated in PHD/RING1 (C84A), PHD/RING2 (C147A), PHD/RING3 (C258A/C261A), and HECT (C666A) domains using standard PCR mutagenesis. Mutant *E6-AP* (T842K/F844N) was also generated by PCR mutagenesis. Wild-type and mutant cDNAs were cloned into pFastBac-Flag-B, a vector derived from pFastBac^{TM}-HT-B vector (Invitrogen) in which the His tag was replaced by 1×FLAG tag (43) (generously provided by Dr. Henbing Wang). All constructs were sequenced to confirm that no unexpected mutations were introduced during cloning. Recombinant bacmids were generated and Sf9 cells were transfected using the Bac-to-Bac baculovirus expression system (Invitrogen) according to the manufacturer's instructions. Sf9 cells expressing recombinant protein were lysed using mammalian cell lysis buffer (50 mM Tris, pH 8.0, 5 mM EDTA, 100 mM NaCl, 10 mM sodium fluoride, 2 mM dithiothreitol, 1 mM Na_3VO_4, 0.5% Nonidet P-40 and proteinase inhibitor mixture (Sigma)). The protein was affinity purified using anti-FLAG M2-agarose beads. The beads were washed three times with mammalian cell lysis buffer and twice with buffer B (50 mM Tris, pH 8.0, 1 mM dithiothreitol) prior to elution with buffer B containing 400 mg/ml 3×FLAG peptide (Sigma).

Ubiquitin Ligase Assay—FLAG-tagged G2E3 fusion proteins were tested for ubiquitin ligase activity in an *in vitro* reaction. Complete reactions contained 100 ng of human E1 (Boston Biochem), 1 μg of E2 (UbcH1, UbcH2, UbcH3, UbcH5a, UbcH7, UbcH9, or UbcH10 (Boston Biochem)), His_6-ubiquitin (Boston Biochem), 1 μg of bacterial lysate (as a surrogate target for ubiquitination), and 1 μg of recombinant FLAG-G2E3 or mutant FLAG-G2E3. Assay buffer contained 50 mM Tris, pH 7.5, 2.5 mM $MgCl_2$, 0.5 mM dithiothreitol, 300 μM ATP, and 1× Energy Regeneration System (Boston Biochem). In some cases, individual reaction components were omitted, as indicated. Reactions were carried out at 30 °C for 1.5 h followed by quenching by boiling in an equal volume of 2× protein sample buffer. SDS-PAGE and immunoblotting were performed as previously described (12).

Generation of G2E3 Mutant Mice—The ES cell line RRM192, derived from 129P2/Ola embryonic stem cells, was purchased from BayGenomics. These cells were generated by electroporation of the trapping construct pGT01xf that contains the En2 splice acceptor upstream of cDNA encoding the β-galactosidase/neomycin resistance fusion protein. ES cells were cultured without feeders in standard M15 medium and microinjected into C57/BL6 blastocysts by the UAB Transgenic Mouse Facility. Four high percentage chimeric founder males were identified by coat color and mated with C57/BL6 females to establish heterozygote animals.

To confirm the identity of RRM192 ES cells, reverse transcriptase-PCR was performed. Total RNA was isolated from cultured ES cells with TRIzol reagent (Invitrogen). cDNA was generated by reverse transcription of 5 μg of total RNA with Moloney murine leukemia virus reverse transcriptase. The first round of nested PCR was conducted with primers exon13S1 (5′-ATGGTGGTCCTTCGCCTGG-3′) and β-galAS (5′-GACAGTATCGGCCTCAGGAAGATC-3′) followed by another PCR with exon13S2 (5′-CTCTACCAACTTTGGATGATGTATCAGAC-3′) and β-galAS.

To determine the vector insertion site within intron 13, a nested PCR approach was used to amplify and clone intron 13 from wild-type and mutant alleles. To clone wild-type intron 13, primers int13S1 (5′-AGGTGGGCATGGTTGAACATG-3′) and int13AS1 (5′-ATGAAAGGCATGCAGCACCAC-3′) were used in an initial PCR followed by amplification with primer pair int13S2 (5′-AGGCTTCAAGGGTAACCTAGACTGC-3′) and int13AS2 (5′-CACTAGATGCAGTCTTAACTATGGAGCC-3′). To clone the mutant allele, the primers int13S1 and vecAS1 (5′-ACGGGTTCTTCTGTTAGTCCCAAC-3′) were used in an initial PCR followed by amplification using primers int13S2 and vecAS2 (5′-CTACATAGTTGGCAGTGTTTGGGG-3′). Each PCR was done with 30 cycles of 94 °C for 30 s, 52 °C for 30 s, and 72 °C for 2 min. Both PCR products were cloned and sequenced.

Genotyping of Mice and Embryos—At weaning, mice were genotyped by Southern blotting or PCR. For Southern blotting, genomic DNA was prepared, digested with PvuII, and separated by agarose gel electrophoresis. After transfer, membranes were probed with a *G2E3* exon 13 probe generated using [^{32}P]dCTP and Megaprime Labeling Kit (Amersham Biosciences) according to the manufacturer's instructions. The wild-type and mutant alleles appear as bands of 6.7 and 2.4 kb, respectively. For genotyping by PCR, genomic DNA was amplified using primers int13F1 (5′-AGGTAAGCATGCTAGATTTTAGAGAGTG-3′) and int13R2 (5′-TCCCACAGGTTCCCCCCC-3′). The wild-type allele generates a PCR product of 132 bp, whereas the mutant allele results in a 68-bp product.

Post-implantation embryos were genotyped by the above described PCR strategy. Vaginal plugs were detected on day E0.5 and embryos were harvested at E8.5, E10.5, or E12.5, and dissected away from uterine tissues. Whole embryos were

digested in proteinase K followed by DNA isolation and PCR. For pre-implantation blastocyst genotyping, lysis was performed in 2 μl of genomic lysis buffer (20 mM Tris, pH 8.0, 100 mM KCl, 4 mM $MgCl_2$, 0.9% Nonidet P-40, 0.9% Triton X-100, and 300 ng/ml proteinase K) followed by heat inactivation of the proteinase K. 1 μl of this lysate was used for nested PCR. For the first PCR, int13F1 and int13R1 (5′-CCAATTCCCACAGGTTCCC-3′) were used with 30 cycles under the same conditions as above. The second PCR was conducted with primers int13F2 (5′-CATGCTAGATTTTAGAGAGTGGGGA-3′) and int13R2 for 35 cycles.

In some cases, blastocysts were subjected to microscopic analysis prior to PCR genotyping. In these cases, the blastocysts were washed with PBS and air dried prior to lysis in 15 μl of genomic lysis buffer. A prolonged heat inactivation for 1 h at 90 °C served to heat inactivate the proteinase K and reverse the fixation. Nested PCR was then performed using 3 μl of this lysate.

Quantitative Real Time PCR—Total RNA was extracted from livers or testes of *G2E3*$^{+/-}$ heterozygotes and wild-type littermates using TRIzol reagent according to manufacturer's recommendations. DNase treatment was used to eliminate genomic DNA contamination and cDNA was synthesized with the SuperScript III reverse transcriptase-PCR kit (Invitrogen). A fragment of the murine *G2E3* cDNA was amplified using SuperScript III Platinum qPCR kit (Invitrogen) and the primer pair 5′-CGTCCAATTCACTCGGTAGCGGACG and 5′-CCATCGTTGTTGCAGATTTACCA. Because these exon 15 and 16 primers are located downstream from the β-geo insertion site, no amplified product should be produced from the mutant transcript. β-Actin was amplified as an internal control. Relative gene expression was calculated from $\Delta\Delta C(t)$ values derived from triplicate determinations of each sample and plotted with standard deviation.

Blastocyst Culture and Staining—To obtain embryonic day 3.5 blastocysts, *G2E3*$^{+/-}$ females were super-ovulated using pregnant mare's gonadotropin (5–7.5 IU/mouse) and hCG (human chorionic gonadotropin, 5–7.5 IU/mouse) and mated with *G2E3*$^{+/-}$ males. On E3.5, uterine horns were flushed with M2 medium (Millipore) and individual blastocysts were harvested for either genotyping or culture. Blastocysts isolated for culture were plated in 24-well plates in 0.5 ml of ES cell medium prepared by supplementing Dulbecco's modified Eagle's medium with 20% fetal bovine serum, 2 mM L-glutamine, 1% β-mercaptoethanol, 1 mM sodium pyruvate, 0.1 mM nonessential amino acids, and 1000 units/ml LIF (Chemicon). For analysis of proliferation, cells were photographed daily using an inverted Nikon phase-contrast microscope. Blastocysts undergoing involution were harvested after 4 days in culture. The remaining blastocysts were harvested after 7 days in culture. Genotyping for all blastocysts was performed by PCR as described above.

To perform TUNEL (TdT-mediated dUTP Nick-End Labeling) staining, blastocysts were first harvested and grown in culture as before. After 3 days in culture, some blastocysts were treated with 300 nM doxorubicin (Sigma) overnight to serve as a positive control for apoptosis. On day 4 of culture, the blastocysts were washed with PBS,[3] fixed in 4% paraformaldehyde, permeabilized with 0.2% Triton X-100, and rinsed with PBS. TUNEL staining was performed using the DeadEnd Fluorometric TUNEL System (Promega) with minor modifications. The blastocysts were pre-equilibrated in labeling buffer for 10 min prior to labeling with the TdT enzyme and fluorescein isothiocyanate-dUTP. The reaction was stopped by addition of 2× SSC and the blastocysts were washed with PBS prior to visualization with a Nikon inverted fluorescence microscope.

To perform Annexin-V staining, blastocysts were harvested at E3.5 and cultured for 3 days. Some blastocysts were treated with doxorubicin (300 nM) overnight prior to Annexin-V staining to serve as positive controls. The medium was aspirated and blastocysts were washed in PBS prior to staining with fluorescein isothiocyanate-Annexin-V (MBL International Corporation). Microscopic analysis was performed as before.

β-Galactosidase Staining of Mouse Embryos—Embryos were harvested from timed pregnant female mice at the indicated day following detection of a vaginal plug and washed in PBS. Embryos were then fixed in LacZ fixative (1% formaldehyde, 0.2% glutaraldehyde, 2 mM $MgCl_2$, 5 mM EGTA, 0.02% Nonidet P-40 in PBS) for 1 h at 4 °C. Three 20-min washes were conducted in PBS. Embryos were stained in LacZ staining solution (5 mM potassium ferricyanide, 5 mM potassium ferrocyanide, 2 mM $MgCl_2$, 0.01% sodium deoxycholate, 0.02% Nonidet P-40, 1 mg/ml 5-bromo-4-chloro-3-indolyl-β-D-galactopyranoside (X-gal) in PBS) in the dark overnight at 37 °C. Embryos were then washed and stored in PBS. For adolescent tissues, 4-week-old heterozygous mice were sacrificed and the indicated organs were dissected and stained as described above. For histological sections, LacZ-stained embryos were embedded in paraffin or snap frozen in OCT, sectioned, and stained with Nuclear Fast Red (Vector Laboratories). Slides were mounted with permount (Fisher).

RESULTS

G2E3 Is a Dual Function Ubiquitin Ligase—G2E3 has four domains that might function in ubiquitin ligation including three RING-like domains in the N-terminal half of the protein and one HECT domain in the C terminus, shown schematically in Fig. 1*A* and in a previous publication (19). Because all three RING-like domains share some similarity to both PHD and RING domains, we refer to them collectively as PHD/RING domains and specifically as G2E3$^{(PHD/RING1)}$ (residues 81–127), G2E3$^{(PHD/RING2)}$ (residues 144–192), and G2E3$^{(PHD/RING3)}$ (residues 238–285). G2E3$^{(PHD/RING1)}$ is most similar to the PHD domain consensus, G2E3$^{(PHD/RING2)}$ is most similar to the prototypic RING domain, and G2E3$^{(PHD/RING3)}$ matches the consensus sequence for both domains poorly. To test whether G2E3 could function as an ubiquitin ligase *in vitro*, we prepared FLAG-tagged G2E3 using a baculovirus expression system. This recombinant protein was tested for its ability to ubiquitinate surrogate target proteins (a bacterial lysate) in a reaction with one of several different E2s (ubiquitin-conjugating enzymes), and epitope-tagged ubiquitin. G2E3 is very active

[3] The abbreviations used are: PBS, phosphate-buffered saline; CNS, central nervous system; E, embryonic.

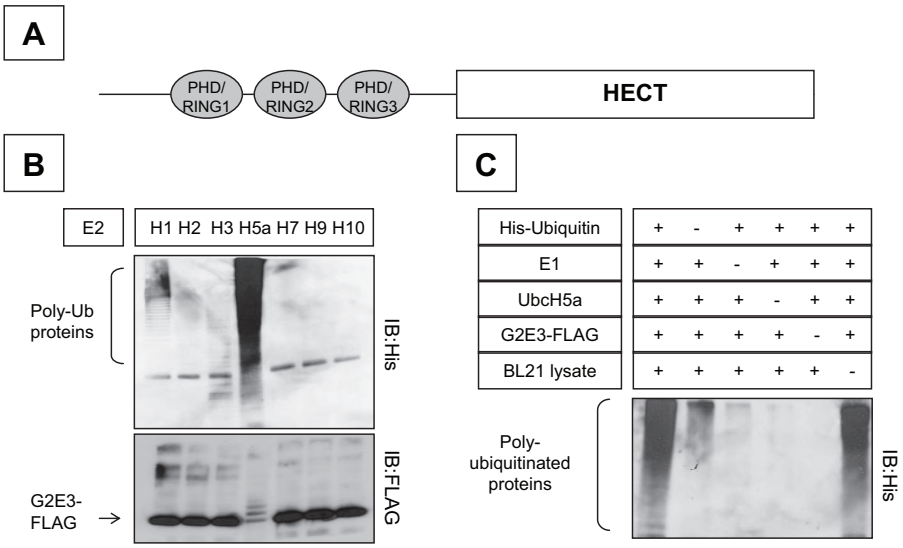

FIGURE 1. **G2E3 functions as an ubiquitin ligase.** *A*, a schematic diagram of G2E3 shows three domains similar to both PHDs and RINGs as well as a C-terminal HECT domain. *B*, recombinant G2E3-FLAG was prepared and purified using a baculovirus expression system. The ability of G2E3-FLAG to mediate polyubiquitination was tested using His-ubiquitin, E1, and one of several E2s as indicated. After incubation at 30 °C for 1.5 h, the reaction was denatured in SDS-PAGE loading buffer, separated by SDS-PAGE, and subjected to immunoblotting with an anti-His antibody. *C*, ubiquitination reactions were performed as before using His-ubiquitin, E1, UbcH5a, and G2E3-FLAG (*first lane*). Similar reactions with a single reaction component omitted were also performed. Polyubiquitination was detected using immunoblotting for anti-His.

in catalyzing polyubiquitination in concert with UbcH5a (Fig. 1*B*, *upper panel*). Very little or no activity is observed with UbcH1, UbcH2, UbcH3, UbcH7, UbcH9, or UbcH10. The recombinant G2E3 is completely converted to higher molecular weight forms in the reaction with UbcH5a, indicating that the protein is autoubiquitinated (Fig. 1*B*, *lower panel*). We next tested whether all reaction components were required for G2E3 to function as an ubiquitin ligase. Using UbcH5a as the E2, no polyubiquitination was observed if either ubiquitin, E1, E2, or G2E3-FLAG was excluded from the reaction mixture (Fig. 1*C*), indicating that the ubiquitination we observed is dependent on all components of the ubiquitination cascade. Polyubiquitination does not require inclusion of the bacterial lysate, again demonstrating that G2E3 is capable of autoubiquitination *in vitro*, as previously observed for many other E3s (examples include those described in Refs. 44–47).

Because there are four potential ubiquitin ligase domains in G2E3, we made recombinant mutated versions of the protein to define the domain(s) responsible for ubiquitination. Cysteines to be mutated were chosen based upon homology to other PHD and RING domains. A schematic representation of each mutant is shown in Fig. 2*A* with a bold X indicating domains inactivated by point mutation. For example, one mutant (PHD/RING1-only) has C → A (cysteine to alanine) mutations to inactivate PHD/RING2, PHD/RING3, and HECT domains. Similar mutants have point mutations that inactivate all domains other than PHD/RING2 (PHD/RING2-only mutant), PHD/RING3 (PHD/RING3-only mutant), or the HECT domain (HECT-only mutant). The catalytic activity of each of these mutants was compared with a negative control mutant bearing mutations of all four domains (mutant 5C → A) and positive control wild-type protein (Fig. 2*B*). In assays using UbcH5a as the E2, wild-type G2E3 has strong ubiquitin ligase activity (Fig. 2*B*, *lane 6*), as expected. Strong E3 activity is also observed with the PHD/RING2-only (Fig. 2*B*, *lane 2*) and PHD/RING3-only (Fig. 2*B*, *lane 3*) mutants indicating that both of these domains are capable of functioning as ubiquitin ligases. No activity is observed with PHD/RING1-only (Fig. 2*B*, *lane 1*) or HECT-only mutants (Fig. 2*B*, *lane 4*). The 5C → A mutant has no E3 activity in this assay, confirming that each point mutation completely inactivates the catalytic function of domain in question. We cannot exclude the possibility that PHD/RING1 or HECT domains may be active *in vivo* or with other E2s (ubiquitin-conjugating enzymes) that we have not tested. Because we only tested activity with seven of about 40 known E2s (Fig. 1*B*), it is conceivable that PHD/RING1 and/or HECT domains could still function in the process of protein mono- or polyubiquitination.

The high molecular weight smear that we observed could be either monoubiquitination at multiple sites or polyubiquitination at one or more sites. To distinguish these two possibilities, we repeated the ubiquitination assay using wild-type G2E3 and the two active mutants (PHD/RING2-only and PHD/RING3-only) along with His_6-tagged wild-type ubiquitin, and either His_6-Ubiquitin^{K48R} or His_6-Ubiquitin^{K63R}. Ubiquitination by G2E3 and both mutants is unaffected by the use of Ubiquitin^{K63R} in the assay (Fig. 2*C*), demonstrating that this reaction is not a result of polyubiquitination on this lysine residue. In contrast, ubiquitination by G2E3 and both mutants is completely abrogated by use of Ubiquitin^{K48R} (Fig. 2*C*), indicating that both domains polyubiquitinate by way of lysine 48 ubiquitin linkages. Therefore, G2E3 performs lysine 48-linked polyubiquitination using two distinct catalytic domains (PHD/RING2 and PHD/RING3 domains).

HECT domains typically function as ubiquitin ligases, although some HECT domain proteins may not have this catalytic activity as a result of departures from the HECT consensus near the C terminus of the domain (48). Our experimental data suggest that the G2E3 HECT domain does not function as an E3 (Fig. 2*B*). Furthermore, the G2E3 HECT domain has numerous amino acid residues that do not match the consensus sequence in the E2 binding site (49) and in the C terminus of the domain (48) that might explain this lack of activity. Perhaps more importantly, the sequence near the active site cysteine in G2E3 diverges markedly from the consensus. The highly conserved tripeptide sequence (T*CX*, where *X* is a hydrophobic residue) in most HECT domains is poorly conserved in G2E3 from several species (*e.g.* KCN in humans, KYR in mice, CDA in zebrafish). To test the influence of these amino acid residues on the HECT domain function, we prepared two versions of recombinant E6-AP, a well characterized HECT E3 (44). The first of these (referred to as E6-AP in Fig. 2*D*) is a N-terminal truncation of

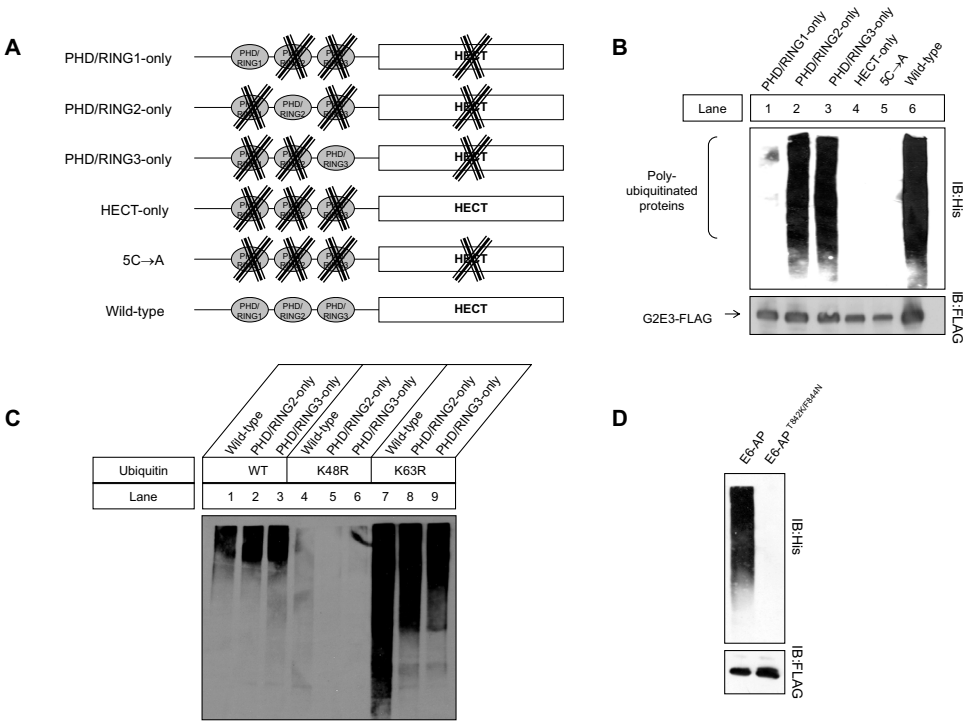

FIGURE 2. **Two PHD/RING domains in G2E3 mediate Lys-48-linked polyubiquitination.** *A*, several mutant versions of G2E3 were prepared by point mutagenesis of cysteines to alanines as described under "Experimental Procedures." The name for each mutant is based on the un-mutated active domain. For example, the PHD/RING1-only mutant has mutations in all domains other than PHD/RING1 (*i.e.* mutations in PHD/RING2, PHD/RING3, and HECT). The mutant name and a schematic of mutated domains are presented with a bold X over inactivated domains. *B*, wild-type and mutant G2E3-FLAG molecules were assayed for ubiquitin ligase activity. Wild-type G2E3 has robust ubiquitin ligase activity (*lane 6*), whereas the negative control (*5C → A*) mutant is devoid of activity (*lane 5*). PHD/RING1-only and HECT-only mutants show no E3 activity (*lanes 1* and *4*, respectively) similar to the negative control. In contrast, both PHD/RING2-only and PHD/RING3-only mutants have ubiquitin ligase enzymatic activity that is comparable with the wild-type protein (*lanes 2* and *3*, respectively). *C*, wild-type G2E3 (*lanes 1*, *4*, and *7*) was compared with PHD/RING2-only (*lane 2*, *5*, and *8*) and PHD/RING3-only (*lanes 3*, *6*, and *9*) mutants for the ability to mediate polyubiquitination using wild-type ubiquitin (*lanes 1–3*), K48R-ubiquitin (*lanes 4–6*), and K63R-ubiquitin (*lanes 7–9*). *D*, wild-type E6-AP and E6-AP bearing two point mutations (T842K/F844N) were produced as FLAG-tagged recombinant proteins using baculovirus. The enzymatic activities of these two recombinant proteins were assayed *in vitro* using His-ubiquitin, E1, UbcH5a, and bacterial lysate as a surrogate target for the polyubiquitination reaction. *IB*, immunoblot.

E6-AP containing the entire HECT domain (residues 545–875 as numbered in NP_000453) and the second (referred to as E6-AP$^{(T842K/F844N)}$ in Fig. 2*D*) differs only by the presence of mutations replacing threonine 842 and phenylalanine 844 with lysine and asparagine, respectively (the residues found in these positions in human G2E3). Although wild-type E6-AP demonstrated robust ubiquitin ligase activity (Fig. 2*D*), mutant E6-AP$^{(T842K/F844N)}$ was completely inactive. This demonstrates that the residues surrounding the active site cysteine are important for ubiquitin ligase function and further shows that the lack of conservation of these residues in G2E3 prevents the domain from functioning as an E3.

Several different sequence motifs have been identified as ubiquitin ligase catalytic domains. The most prevalent of these are the HECT domain (44) and the RING finger (20), a motif with several different subtypes. Another motif identified with E3 activity is the U-box (50), which has considerable similarity to the RING finger. Finally, some PHD domains (another motif that is similar to the RING) appear to function as E3s, but some of these may be more correctly identified as RINGs. Because the two ubiquitin ligase domains in G2E3 bear similarities to both PHDs and RINGs, we performed sequence comparisons to facilitate assignment of each to the RING or PHD family and to identify variations on the consensus sequence that do not eliminate catalytic activity. The second PHD/RING domain from G2E3 most closely matches the consensus for RING domains. In Fig. 3*A*, the sequence of human (Hs) and murine (Mm) G2E3$^{(PHD/RING2)}$ are compared with other RING domains including the classic C_3HC_4 ubiquitin ligase from the IAP1 and Cbl, the alternative $C_3H_2C_3$ seen in ZNRF3 and RNF126, and the much less common and more divergent C_3XHC_3 (represented by MEKK1 and the hypothetical protein H05L14.2) and C_3XC_4 domains (represented by Rbbp6 and Jumonji), where *X* is typically an asparagine or basic residue. A variation on the RING domain seen in some proteins, the C_4HC_3 RING variant (51), differs significantly from other RINGs in amino acid spacing so representatives with this domain organization are not included in this alignment. G2E3$^{(PHD/RING2)}$ from most species including human and mouse match the C_3XHC_3 structure well. RING domains are similar to PHD domains, which has caused ongoing controversy about assignment of some domains to one category or the other (26, 27, 52). In some cases, assignment to one category may be confounded by the presence of another residue that might serve as a zinc coordinating residue. For example, in G2E3 and the other two C_3XHC_3 RINGs shown in Fig. 3*A*, a cysteine (highlighted in *green*) could serve as the third (of eight) zinc coordinating residue, thereby eliminating the role for the *X* residue (shown in *blue*) in this process. In G2E3, its location directly adjacent to the next zinc coordinating residue (see human and mouse G2E3 in Fig. 3*A*) makes it very unlikely that this residue could contribute to zinc binding. In the absence of three-dimensional structural data, these data strongly suggest that *G2E3*$^{(PHD/RING2)}$ is a bona fide RING domain using an atypical residue in a position typically occupied by a cysteine or histidine.

The third PHD/RING domain from G2E3 (G2E3$^{(PHD/RING3)}$) matches the classic RING structure poorly. However, like both PHD and RING-variant (51) domains, it has the C_4HC_3 organization of zinc coordinating residues and shares features with both domains. Using SMART, we have aligned several similar C_4HC_3 PHD (Fig. 3*B*) and RING-variant domains (Fig. 3*C*). Alignment between human (Hs) and murine (Mm) G2E3$^{(PHD/RING3)}$ and other PHD proteins reveal conser-

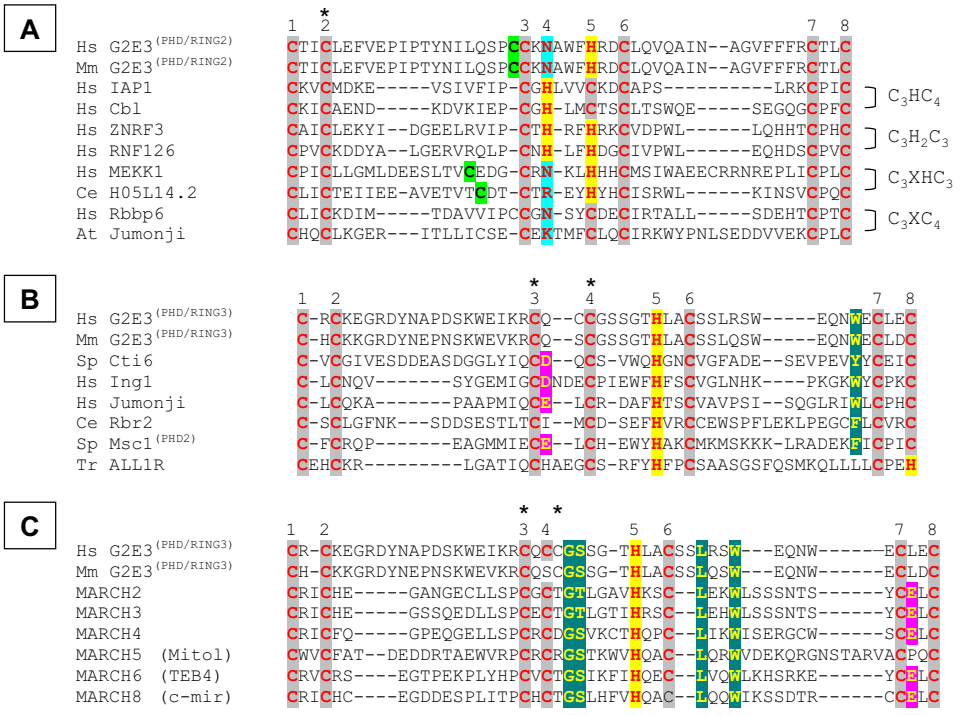

FIGURE 3. **Comparison of G2E3$^{(PHD/RING2)}$ and G2E3$^{(PHD/RING3)}$ domains with RING and PHD domains.** Domains are aligned with residues that are predicted to coordinate zinc are *numbered* and in *red*. These residues are highlighted in *gray* (cysteines), *yellow* (histidines), or *blue* (other residues found at this position). *A*, human (*Hs*) and murine (*Mm*) G2E3$^{(PHD/RING2)}$ are aligned with RINGs from human (*Hs*) proteins IAP1, Cbl, ZNRF3, RNF126, MEKK1, and Rbbp6 as well as *Arabidopsis* retinoblastoma binding protein 6 (*At Rbbp6*) and hypothetical *C. elegans* protein (*Ce H05L14.2*). The first three and the last three zinc coordinating residues are all cysteines, whereas the *middle two* are a combination of cysteines (*C*), histidines (*H*), or other (*X*) residues. G2E3$^{(PHD/RING2)}$ is very similar to the C_3XHC_4 pattern like that seen in MEKK1 and H05L14.2. Conserved cysteines in MEKK1 and H05L14.2 that might be predicted to coordinate zinc according to the alternative RING consensus are highlighted in *green*. Similar conserved cysteines in human and murine G2E3 are also highlighted in *green*. The cysteine mutated in G2E3 to render PHD/RING2 inactive (C147) is indicated by an *asterisk*. *B*, human (*Hs*) and murine (*Mm*) G2E3$^{(PHD/RING3)}$ are aligned with PHDs from human (*Hs*) Cti6 and Jumonji, *C. elegans* retinoblastoma-related protein 2 (*Ce Rbr2*), *S. pombe* multicopy-suppressor of Chk1 (*Sp Msc1*), and *Takafugu rubripes* ALL-1 related protein (*ALL1R*) domain proteins. The PHD from Msc1 is a confirmed ubiquitin ligase. A conserved aromatic residue is *yellow* highlighted in *teal*. The two cysteines mutated to render PHD/RING3 inactive (Cys-258 and Cys-261) are indicated by *asterisks*. *C*, human (*Hs*) and murine (*Mm*) G2E3$^{(PHD/RING3)}$ are aligned with RING-variant domains from several known ubiquitin ligases from the membrane-associated RING-CH1 family. Several conserved residues are in *yellow* and highlighted in *teal*. The cysteines mutated to render PHD/RING3 inactive are again indicated by *asterisks*.

vation of zinc binding residues, the presence of an aromatic residue (in *yellow* and highlighted in *teal*) at position −2 relative to the seventh zinc binding residue, and the presence of a single residue between cysteines 1 and 2 of the domain, common in PHD domains. The spacing between several zinc coordinating residues in G2E3$^{(PHD/RING3)}$ is unusual, but in all cases, a similar spacing pattern is found in some other PHDs (refer to Fig. 3*B*). For example, the long spacing between coordinating residues 2 and 3 is shared with Cti6, and the five (rather than the typical four) residues between 4 and 5 and the relatively shorter spacing between 6 and 7 are shared with Ing1. A conserved acidic residue (highlighted in *pink*) that is frequently present in PHDs is absent in G2E3$^{(PHD/RING3)}$ and some other PHDs including those from retinoblastoma-related protein 2 (Rbr2) and ALL-1-related protein (ALL1R).

Although G2E3$^{(PHD/RING3)}$ also share similarities with the RING-variant domain (Fig. 3*C*) found in several members of the MARCH (membrane associated RING-CH) protein family (51), it also is significantly different from this version of the RING. Shared features include the overall C_4HC_3 arrangement for the domain from human and some other species and the presence of several highly conserved residues highlighted in *teal*. The presence of a single amino acid residue between cysteines 1 and 2 and the presence of six (rather than the otherwise completely conserved seven) residues between cysteine 4 and the histidine in position 5 are very atypical. Perhaps most importantly, the fourth zinc-coordinating cysteine residue in this alignment is not conserved in G2E3 from mouse and many other species. An acidic residue found in almost all RING-variant domains highlighted in *pink* is not found in G2E3$^{(PHD/RING3)}$. Therefore, whereas G2E3$^{(PHD/RING3)}$ clearly has ubiquitin ligase activity (Fig. 2*B*), it appears to be more similar to the PHD consensus (Fig. 3*B*) than the RING-variant consensus (Fig. 3*C*). However, unambiguous assignment as a PHD (which infrequently have E3 activity) or RING domain (which usually have E3 activity) will require three-dimensional structural analysis. Nonetheless, the catalytic activity displayed by this unusual domain demonstrates that proteins that do not closely match RING or PHD consensus sequences may still have E3 activity.

The BayGenomics Clone RRM192 Specifically Targets the G2E3 Locus—To assess the *in vivo* function of G2E3, we have developed a knock-out mouse model of *G2E3* inactivation. We obtained commercially available ES cells (BayGenomics clone RRM192) with an insertional mutation in the *G2E3* locus. Reverse transcriptase-PCR with primers specific for exon 13 of *G2E3* and β-galactosidase allowed us to clone a copy of the mutant cDNA. Sequencing confirmed that the *G2E3* gene was disrupted as reported by BayGenomics.

To determine the genomic insertion site, nested PCR was performed using primers within exon 13 and antisense primers annealing to the 5′ end of the insertion vector sequence. Using genomic DNA from RRM192 cells as a template, a PCR product similar to the expected size was generated, cloned, and sequenced. We found that the insertion lies ~570 base pairs downstream from the end of exon 13, disrupting the HECT domain. We also found that 64 nucleotides from intron 13 just upstream of the insertion were deleted in the mutant allele, presumably as a result of the recombination event. A diagram in Fig. 4*A* shows the domains of the G2E3 protein and the portion of the HECT domain that is deleted by insertion between exons 13 and 14. Diagrams of the wild-type allele (Fig. 4*A*), the target-

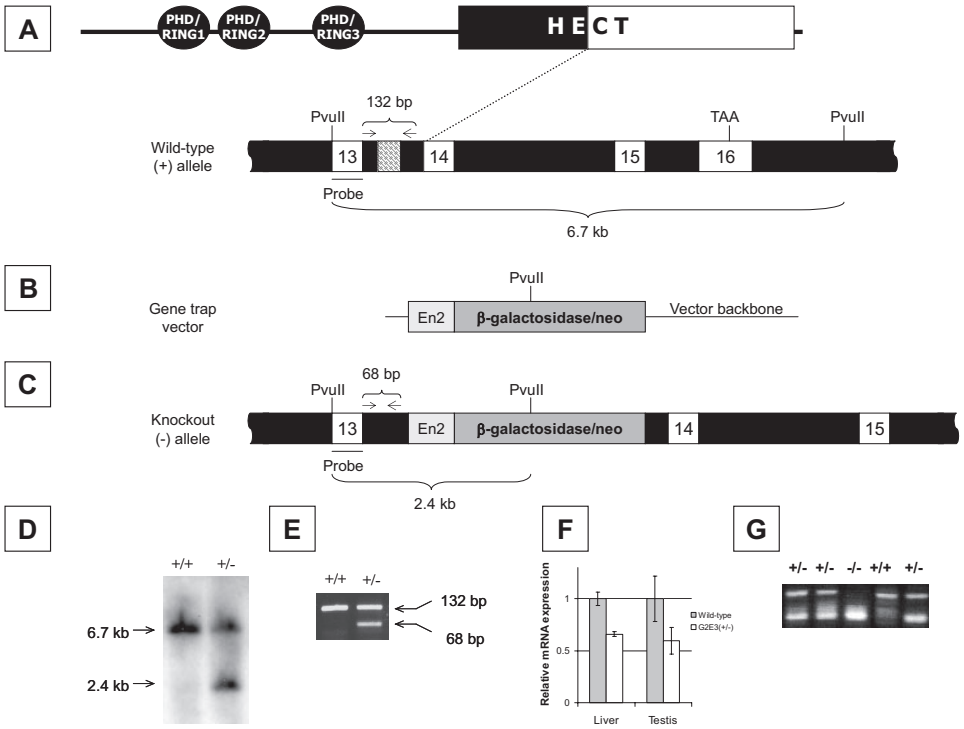

FIGURE 4. ***G2E3* gene disruption and identification of mutant alleles.** *A*, G2E3 has three N-terminal PHD/RING domains and a C-terminal HECT domain. Most of the HECT domain is deleted by the targeting construct insertion between exons 13 and 14. The intron-exon organization of the 3′ end of the wild-type murine *G2E3* gene is shown schematically. PvuII restriction sites are found in the 5′ end of exon 13 and in the intron following exon 16. *B*, a schematic of the pGT01xf trapping construct. A PvuII site is shown within the β-geo cDNA. *En2*, engrailed 2 splice acceptor; *neo*, neomycin resistance gene. *C*, intron-exon organization of the 3′ end of the trapped *G2E3* allele. 64 bp are absent from intron 13 near the site of the insertion. *D*, PvuII-digested genomic DNA from homozygous wild type (+/+) or heterozygous (+/−) mice were Southern blotted with a cDNA probe to exon 13. The wild-type allele results in a band of ~6.7 kb, whereas the trapped allele generates a 2.4-kb DNA fragment. *E*, PCR of wild-type or heterozygous DNA using primers that flank the 64-bp deletion of the trapped intron 13 allow determination of genotype. The wild-type allele generates a 132-bp fragment, whereas the trapped allele generates a 68-bp fragment. *F*, quantitative PCR analysis of full-length *G2E3* expression in wild-type or heterozygous mice. Primers to amplify a portion of exons 15 and 16 were used for the quantitative PCR. The liver of female mice and the testes of male mice were used in this analysis. All 4 animals were littermates. Expression of full-length *G2E3* is decreased ~40% in the heterozygous mice. *G*, genomic DNA was isolated from E3.5 blastocysts from heterozygous matings and PCR amplified by a nested PCR approach described under "Experimental Procedures." Homozygous mutant blastocysts were found to be in the same proportion as homozygous wild-type embryos indicating that *G2E3*$^{-/-}$ blastocysts are viable at E3.5.

TABLE 1

Genotype distribution of offspring from *G2E3*$^{+/-}$ intercrosses at indicated stages

Age[a]	Total (litters)	Genotype[b]		
		+/+	+/−	−/−
E3.5[c]	37	7 (19%)	22 (59%)	8 (22%)
E8.5	34 (6)	11 (32%)	23 (68%)	0
E10.5	21 (3)	8 (38%)	13 (62%)	0
E12.5	15 (3)	4 (27%)	11 (73%)	0
3 weeks	196 (38)	62 (32%)	134 (68%)	0

[a] Animals from heterozygous intercrosses were harvested at the indicated embryonic day or at 3 weeks after birth.
[b] Genotypes were determined by single PCR or Southern blot for post-implantation embryos and 3-week-old mice and by nested PCR for E3.5 blastocysts as described under "Experimental Procedures."
[c] All blastocysts that were genotyped exhibited normal morphology.

ing vector (Fig. 4*B*), and the mutant allele (Fig. 4*C*) show the arrangement of exons, PvuII sites used for screening, and the location of the small deletion of intron 13 present in the mutant allele. Southern blotting of genomic DNA digested with PvuII allows distinction of wild-type and mutant alleles using an exon 13 probe. The wild-type allele produces a 6.7-kb band hybridizing to the exon 13 probe (Fig. 4. *A* and upper band in *D*), whereas the mutant allele produces a 2.4-kb band (Fig. 4, *C* and *lower band* in *D*). The presence of the small (64 nucleotide) deletion in intron 13 also allows screening by PCR, because the wild-type allele generates a 132-bp product (Fig. 4, *A* and *upper band* in *E*) and a 68-bp product is generated by the mutant allele (Fig. 4, *C* and *lower band* in *E*).

G2E3 Disruption Causes Massive Apoptosis and Early Embryonic Lethality—Following confirmation of the mutation in the RRM192 ES cells, they were microinjected into C57BL/6 blastocysts and implanted into the uteri of pseudopregnant female mice. Four chimeric males were identified by coat color and were bred with C57BL/6 females to produce *G2E3*$^{+/-}$ heterozygous animals. As an independent confirmation of the gene disruption, we performed quantitative PCR on RNA from *G2E3*$^{+/-}$ heterozygotes and wild-type littermates. We found that heterozygous animals express ~40% less *G2E3* mRNA than wild-type animals (Fig. 4*F*), consistent with disruption of one *G2E3* allele, perhaps with some compensatory increase in expression from the remaining normal allele. Adult heterozygotes were fertile and had no apparent change in longevity. To generate homozygous mutant mice, we intercrossed heterozygous animals and genotyped offspring at weaning. Surprisingly, no homozygous mutant animals were found among the 196 mice analyzed. Although occasional perinatal deaths were observed, no homozygous knockouts were identified among those animals. Wild-type and heterozygous animals were found to occur at the 1:2 Mendelian ratio (32% wild type, 68% heterozygous) expected for an embryonic lethal phenotype (Table 1).

To determine the time at which lethality occurs, we set up timed pregnancies and harvested embryos at three different stages of development for genotyping. No homozygous mutant animals were found as early as 8.5 days post-coitum. As shown in Table 1, the ratios of wild-type to heterozygous mice at each stage were maintained at ~1:2 (E12.5, 27% WT, 73% heterozygote; E10.5, 38% WT, 62% heterozygote; E8.5, 32% WT, 68% heterozygote). We also noticed a lack of resorption sites from E8.5 litters that are commonly seen in knock-out animals that die following implantation, indicating that the homozygous knock-out embryos likely die very early in development. To assess whether embryos survive until the blastocyst stage, we

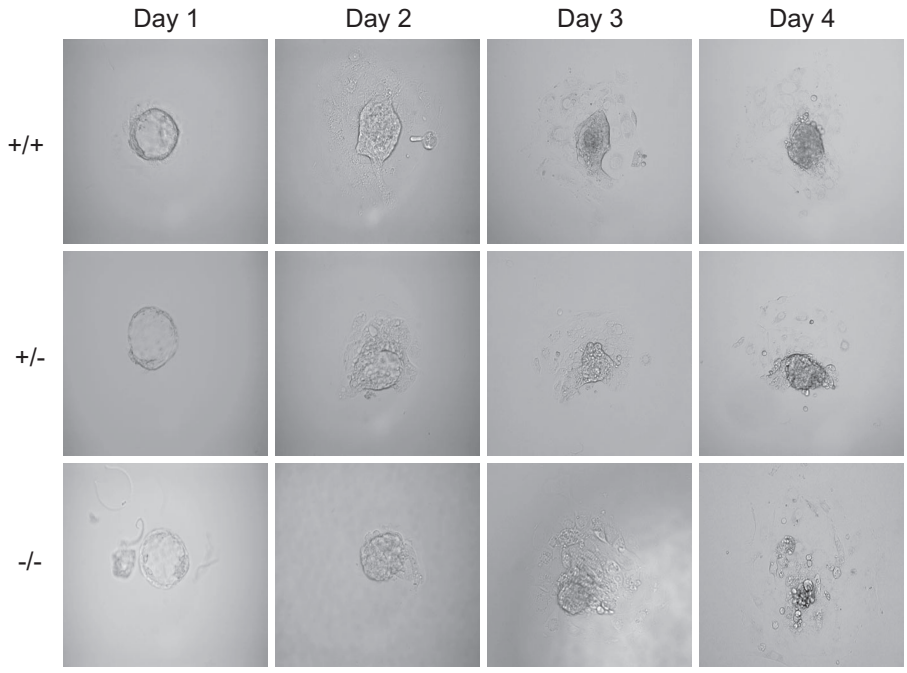

FIGURE 5. ***G2E3* null blastocysts fail to proliferate in culture and undergo involution.** Blastocysts harvested at E3.5 were cultured in ES cell medium and then photographed using phase-contrast microscopy daily for 4 days. Both wild-type (*top row*) and heterozygous blastocysts (*middle row*) continue to proliferate normally, whereas *G2E3* null blastocysts begin to appear overtly abnormal by day 3 in culture and have undergone nearly complete involution by Day 4.

isolated E3.5 blastocysts and genotyped them by nested PCR, as shown in Fig. 4*G*. Of 37 total blastocysts genotyped, 7 were wild-type, 22 were heterozygotes, and 8 were homozygous mutants. This approximates the expected 1:2:1 Mendelian ratio indicating that homozygous *G2E3* inactivation does not impair viability at E3.5.

To define the defect leading to embryonic lethality, we cultured blastocysts to determine whether G2E3 deficiency impaired cell proliferation or viability. Blastocysts from timed pregnancies were harvested at E3.5 and plated in ES cell medium for blastocyst propagation. Twenty-five blastocysts attached to cell culture wells and hatched from the zona pellucida. Photomicrographs of blastocysts were obtained daily beginning 1 day after plating (Fig. 5). No appreciable differences were noted for the first 2 days of culture, but involution of seven of the blastocysts was first noted on day 3. In involuted blastocysts, almost all of the inner cell mass was lost by the fourth day of culture, at which time the remaining cells were harvested for genotyping. The surviving blastocysts were propagated for 3 additional days. There was no further blastocyst death during that period, so these remaining cultured blastocysts were harvested at that time (7 days of culture) for genotyping. Of the 18 blastocysts that survived and proliferated through day 7 of culture, 7 were wild-type, 11 were $G2E3^{+/-}$, and none were $G2E3^{-/-}$. Of the seven blastocysts that failed to proliferate, six were confirmed to be $G2E3^{-/-}$ homozygotes, whereas the seventh could not be genotyped because inadequate DNA was harvested. The proliferation of wild-type and heterozygous blastocysts and the involution of the $G2E3^{-/-}$ blastocysts is shown in Fig. 5.

The abrupt demise of blastocysts in culture suggested that they were dying as a result of apoptosis. To test this, we first analyzed the blastocysts to determine whether the $G2E3^{-/-}$ blastocysts were TUNEL-positive, an established marker of apoptosis (53). Blastocysts were harvested at E3.5 and cultured as before. After 2 days in culture, some blastocysts were treated with the DNA damaging agent doxorubicin (300 nM) to serve as a positive control for apoptosis. Cells were fixed and assayed for TUNEL status after a total of 3 days in culture. As expected, doxorubicin treatment caused a large fraction of the cells in the blastocysts to undergo apoptosis, as evidenced by TUNEL-positivity (Fig. 6*A*, *bottom row*). Most untreated blastocysts showed virtually no TUNEL-positive cells. Genotyping confirmed that these TUNEL-negative blastocysts were either wild-type or heterozygous for the *G2E3* knockout, as shown for representative blastocysts in the first and second rows of Fig. 6*A*. A fraction of untreated blastocysts were overtly TUNEL-positive despite having a markedly decreased inner cell mass. Genotyping confirmed that these blastocysts were homozygous knockouts, as shown for a representative knock-out blastocyst in the *third row* of Fig. 6*A*. This result demonstrates that complete inactivation of *G2E3* leads to embryonic lethality as a result of apoptosis prior to implantation.

As an independent confirmation of the role of G2E3 in preventing embryonic apoptosis, we performed Annexin-V staining of cultured blastocysts, another well established method of identifying apoptotic cells (53). Blastocysts were harvested and cultured as before. After 3 days of culture, the blastocysts were stained with Annexin-V. As expected, the $G2E3^{-/-}$ blastocysts were Annexin-V positive similar to doxorubicin-treated positive controls, whereas wild-type and heterozygous blastocysts were negative (Fig. 6*B*), confirming that G2E3 is required for prevention of apoptotic death in early embryogenesis.

Because p53 plays a pivotal role in many apoptotic responses, we considered the possibility that p53 might be required for apoptosis initiated by G2E3 inactivation. We established double heterozygotes for *G2E3* and *p53* (*i.e.* $G2E3^{+/-}p53^{+/-}$ mice) to assess whether inactivation of *p53* might rescue the lethal phenotype associated with *G2E3* inactivation. Despite many interbreedings between several double heterozygotes, no $G2E3^{-/-}p53^{-/-}$ or $G2E3^{-/-}p53^{+/-}$ were obtained (data not shown). This suggests that cell death caused by *G2E3* inactivation does not require *p53*.

G2E3 Is Expressed in the Developing CNS—Because homozygous inactivation of *G2E3* causes early embryonic death, we are unable to examine its function later in development. Therefore, analysis of expression in heterozygous mice is particularly important to gain more information about potential functions

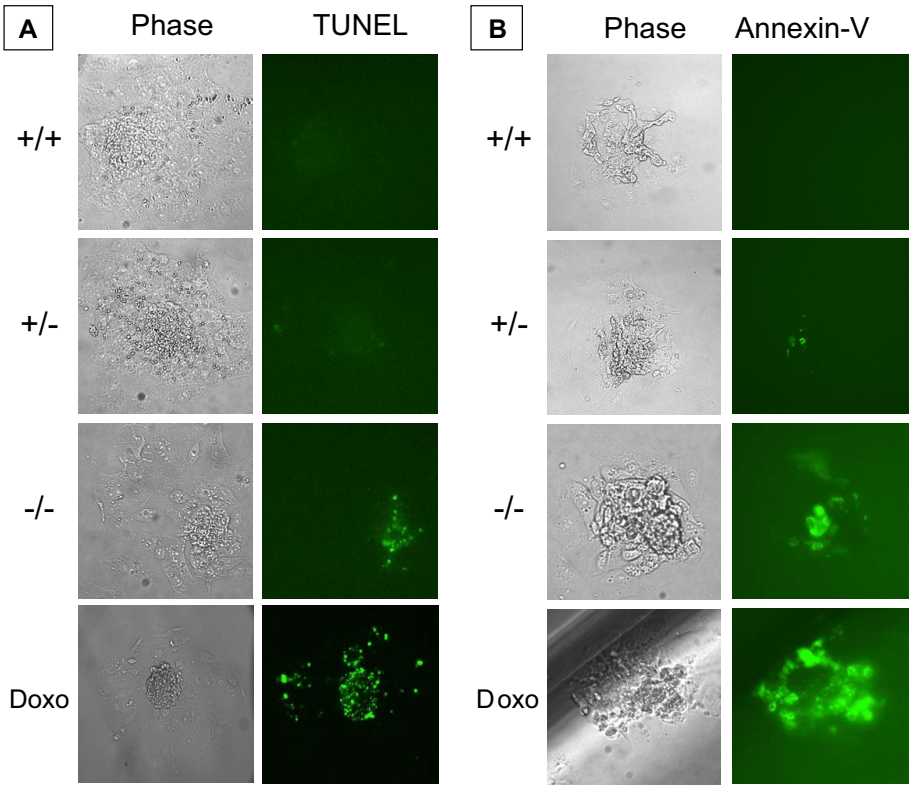

FIGURE 6. ***G2E3* null blastocysts undergo apoptosis.** *A*, blastocysts harvested at E3.5 were cultured for 3 days and then fixed prior to TUNEL staining to identify apoptotic cells. As a positive control, blastocysts were treated with doxorubicin overnight prior to staining. Blastocysts were analyzed by phase-contrast microscopy and fluorescence microscopy to identify TUNEL-positive cells. After staining, PCR genotyping was performed. Wild-type (+/+) and heterozygous (+/−) blastocysts showed almost no TUNEL-positive cells. In contrast, homozygous knock-out (−/−) blastocysts showed TUNEL-positivity similar to doxorubicin-treated blastocysts. *B*, blastocysts were harvested at E3.5 and cultured as before. After 3 days in culture, blastocysts were stained with Annexin-V to identify apoptotic cells. After microscopic analysis using phase-contrast and fluorescence microscopy, PCR genotyping was performed. Almost no Annexin-V-positive cells were identified in wild-type (+/+) and heterozygous (+/−) blastocysts, whereas overt positivity similar to that for the doxorubicin-treated positive control is observed in homozygous knock-out (−/−) blastocysts.

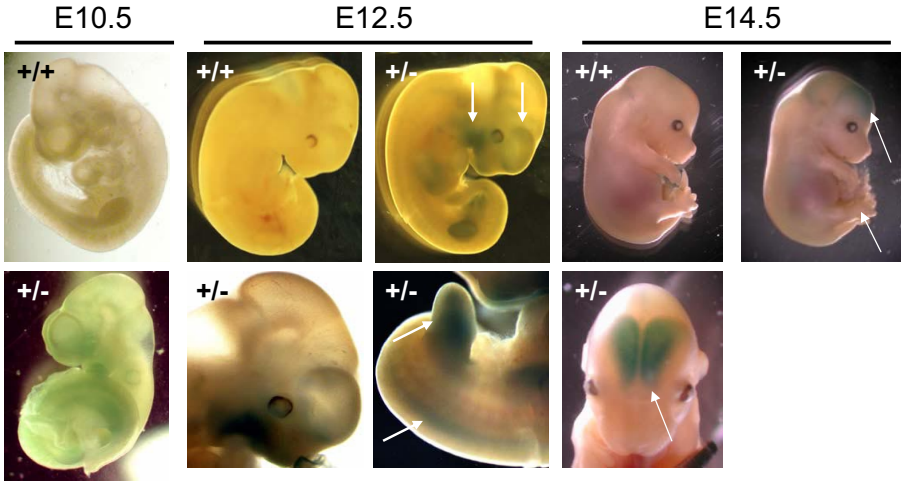

FIGURE 7. **G2E3 expression in the CNS and limb buds during embryogenesis.** Embryos were harvested at the indicated days from timed pregnancies of heterozygous intercrosses. These were then fixed and stained as described under "Experimental Procedures." Whole mount embryos were imaged for β-galactosidase staining. Wild-type embryos displayed no staining, whereas heterozygous animals stained *bluish green* in tissues expressed high levels of G2E3. The most intense staining was observed in the forebrain, neural tube, and limb buds.

of this ubiquitin ligase. An advantage of using gene trap constructs containing the β-galactosidase marker is sensitive identification of tissues that express the gene into which the targeting vector is inserted. Insertion of the vector within intron 13 of murine *G2E3* results in a protein fusion of the first 13 exons of *G2E3* with the β-galactosidase reporter gene under control of the endogenous promoter for *G2E3*. This allows for sensitive identification of tissues and cell types that express *G2E3* by assaying β-galactosidase activity.

Embryos derived from timed pregnancies from heterozygous crosses were harvested, fixed, and assayed for β-galactosidase activity at different stages of development (Fig. 7). At E12.5, we observed intense staining within the forebrain, neural tube, brachial arch, and limb buds, as marked by *arrows*. Diffuse staining was also observed within the abdomen. A similar pattern was seen in E10.5 embryos, although the staining intensity was greatly diminished suggesting that *G2E3* mRNA expression is lower at this stage of development. We also analyzed the expression pattern at E14.5 and observed the most intense β-galactosidase activity within the forebrain (marked by *arrows*) with additional staining in the midbrain, spine, and abdomen. In contrast to the limb buds of E12.5 embryos, the patterned limbs of E14.5 embryos showed no detectable staining, indicating a potential role for G2E3 in limb patterning processes. The lack of staining in the E14.5 limb is indicated by an *arrow*.

We prepared paraffin and frozen sections of E12.5 heterozygote embryos and analyzed β-galactosidase staining by light microscopy. Within the embryonic tissues, staining is observed in the forebrain (Fig. 8, *A* and *B*), corresponding with the prominent staining seen by whole mount (Fig. 7). Adjacent sagittal slices stained with β-galactosidase (Figs. 8*A*) and Nuclear Fast Red (Fig. 8*B*) are shown to allow comparison of β-galactosidase staining and CNS architecture. Sagittal sections through the developing ventricular system demonstrate staining within the ependymal cells lining the ventricles and the underlying nervous tissue (Fig. 8, *C*–*E*). A coronal section further indicates staining within the ependymal

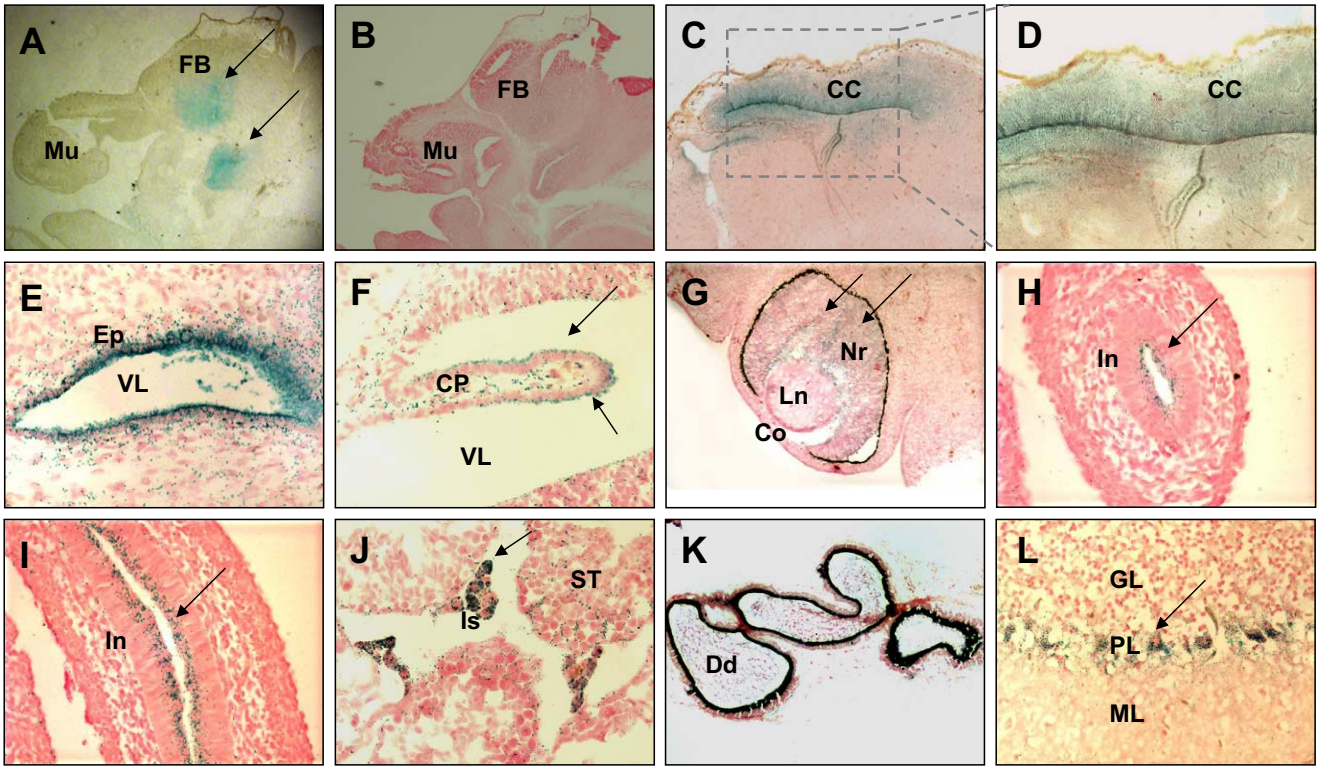

FIGURE 8. **Histology of β-galactosidase-stained embryos and tissues.** E12.5 heterozygous embryos or adolescent brain and testis were assayed for β-galactosidase activity as described under "Experimental Procedures." Subsequently, they were snap frozen (*A–E* and *G–L*) or paraffin embedded (*F*) and sectioned. β-Galactosidase (*A* and *C–L*) or Nuclear Fast Red (*B–L*) staining is shown. *A* and *B*, sagittal sections of E12.5 embryos were stained with or without Nuclear Fast Red. Muzzle and head are shown. *C–E*, the developing ventricles are shown under low, medium, or high power magnification. *F*, a coronal section of E12.5 embryo demonstrates staining in the ependymal cells of the choroid plexus. *G*, sagittal section of the eye indicates expression of G2E3 within the neural retina. Cross (*H*) or longitudinal (*I*) sections of the developing intestine demonstrate expression within the epithelial cells of the lumen are shown. *J*, cross-section of 4-week-old testis with staining of the interstitial cells and mild staining of the seminiferous tubules. *K*, cross-section of ductus deferens exhibits intense staining within the apical epithelium. *L*, cross-section of the adult brain with staining within the Purkinje cell layer. *Mu*, muzzle; *FB*, forebrain; *CC*, cerebral cortex; *Ep*, ependyma; *VL*, ventricle lumen; *CP*, choroid plexus; *Co*, cornea; *Ln*, lens; *Nr*, neural retina; *In*, intestine; *Is*, interstitial cells; *ST*, seminiferous tubules; *Dd*, ductus deferens; *GL*, granular layer; *PL*, Purkinje layer; *ML*, molecular layer.

cells of the choroid plexus (Fig. 8*F*). Staining of E12.5 embryos also reveals faint diffuse β-galactosidase staining in one other CNS structure, the developing retina (Fig. 8*G*). Outside of the CNS, one area of discrete staining was noted in cells lining the embryonic intestine (Fig. 8, *H* and *I*).

We further analyzed the expression of G2E3 in adolescent mice. Frozen sections of brain, testis, kidney, heart, liver, spleen, and pancreas were examined for detectable G2E3 protein expression. No measurable β-galactosidase staining could be seen within the tissues of any organ with the exception of brain and testis. The Purkinje cell layer of the cerebellum exhibited high levels of G2E3 but no other nervous tissue demonstrated measurable expression (Fig. 8*L*). Notably, expression of the mutant protein appears to be restricted to the cytoplasm in contrast to the wild-type protein that is concentrated within the nucleus. This is just as expected, because C-terminal deletions of the G2E3 HECT domain (like those in this mutant G2E3/β-galactosidase fusion protein) have been shown to cause mislocalization of the protein to the cytoplasm (19). Within the testicles, the interstitial cells demonstrated expression of G2E3 but only minimal staining is observed in the surrounding seminiferous tubules (Fig. 8*J*). Additionally, very intense staining is seen in the apical cells of the ductus deferens (Fig. 8*K*).

DISCUSSION

In this study, we characterize the cell cycle-regulated ubiquitin ligase known as G2E3, demonstrating its biochemical function, physiologic function, and its *in vivo* expression pattern. We first demonstrate that G2E3 is an ubiquitin ligase by virtue of two distinct domains, including both a RING domain and an atypical domain with similarities to both RING variant and PHD domains. Surprisingly, a HECT domain in G2E3 appears to lack catalytic activity, at least in part as a result of residues that surround the active site cysteine. The HECT domain has previously been shown to play an important role in G2E3 subcellular localization (19). To our knowledge, this is only the second protein (and the first mammalian protein) with two distinct E3 domains, a feature first shown for the yeast protein Msc1 (22). The presence of two distinct ubiquitin ligase domains on a single protein might be expected to allow ubiquitination of distinct targets by each domain and could conceivably allow regulation of each domain by the other. Identification of *in vivo* targets of each ubiquitin ligase domain will be an interesting future goal, especially given the great importance of this protein in embryogenesis.

We further show that G2E3 plays an essential role in early embryonic development. Disruption of *G2E3* is lethal at a very early stage in development and deficiency of the protein causes

massive apoptosis with resulting involution of the blastocyst. The embryonic apoptosis seen with G2E3 deficiency is similar to that observed with deficiency of the G2E3 ortholog from *Drosophila* known as *pineapple eye* (54). Despite the cell cycle-regulated expression of G2E3 (4), knock-out blastocysts do not undergo a mitotic arrest (data not shown), just as was shown for *pineapple eye*. Although some cell cycle and checkpoint proteins are also essential in embryogenesis, many are dispensable, likely as a result of compensation by similar proteins. For example, disruption of one or two *Cyclin D* genes leads to embryologic defects in some organs (55), and inactivation of all three causes embryonic demise late in gestation (56). In contrast, the embryonic lethality observed with inactivation of *G2E3* indicates that it cannot be fully compensated for by NYD-SP6, a protein with significant homology to the N-terminal half of G2E3 (57). Two other mitotic regulatory proteins, *Emi1* (29) and *Cdk11* (30), display early embryonic lethality with accompanying mitotic defects in blastocysts. One other ubiquitin ligase, EDD, also is essential in development, reinforcing the importance of this protein modification in mammalian biology (58).

The insertional mutagenesis in the *G2E3* allele produces a fusion transcript that deletes more than half of the HECT domain. Although it is possible that truncation of the HECT domain of G2E3 causes the mutant protein to function as a dominant-negative, this is extremely unlikely because no phenotype is observed in heterozygous animals. Instead, the protein is functionally inactivated by one or more mechanisms. From previous work, we know that C-terminal deletions of the HECT domain (like those present in the protein product from the insertional mutagenesis allele) cause mis-localization of the protein to the cytoplasm rather than the nucleus, its normal site of accumulation (19). As shown in Fig. 8*L*, the aberrant subcellular localization is also seen in Purkinje cells, a further confirmation of the effect of this insertional mutagenesis on subcellular localization of the protein. Mis-localization of G2E3 to the cytoplasm would be expected to prevent it from ubiquitinating target proteins in the nucleus, thereby functionally inactivating the protein. Although other factors could contribute to inactivation of the G2E3 in this insertional mutagenesis, mis-localization alone could easily be expected to render G2E3 nonfunctional as an E3 for specific target protein(s).

The embryonic expression pattern of G2E3 suggests roles for the protein in development of the central nervous system and in limb formation. The function of G2E3 in these processes is likely distinct from its role in early embryonic development, because *G2E3* null embryos die prior to the initiation of organogenesis. With the present data, we can only speculate about the role of G2E3 in CNS and limb development. The abrupt cessation of G2E3 expression in the limb bud suggests that the protein may function in the process of digitation. We speculate that G2E3 may suppress apoptosis prior to initiation of digitation, based on evidence in flies (54) and mice (Fig. 6, *A* and *B*) demonstrating that *pineapple eye* and *G2E3* inactivation leads to increased apoptosis.

In summary, we have demonstrated that *G2E3* is a dual function ubiquitin ligase that is required for prevention of apoptosis during early embryonic development. Generation of a conditional knock-out mouse model for *G2E3* would greatly enhance our ability to examine the role of this protein in mammalian development and would likely provide further insights into its role in development and cellular function.

Acknowledgments—We thank Wendi Jamison with assistance in performing quantitative PCR, Jinju Zhang for assistance with blastocyst isolation, Brad Yoder and co-workers for assistance with blastocyst imaging and manuscript review, and Hengbin Wang for the pFast-FLAG-B vector and assistance with baculoviral protein production. We also appreciate the help of Daniel Bullard and David Kelly for useful discussions and review of the manuscript.

REFERENCES

1. Sherr, C. J. (1996) *Science* **274,** 1672–1677
2. Sherr, C. J. (2000) *Cancer Res.* **60,** 3689–3695
3. Artus, J., and Cohen-Tannoudji, M. (2008) *Mol. Cell. Endocrinol.* **282,** 78–86
4. Crawford, D. F., and Piwnica-Worms, H. (2001) *J. Biol. Chem.* **276,** 37166–37177
5. Whitfield, M. L., Sherlock, G., Saldanha, A. J., Murray, J. I., Ball, C. A., Alexander, K. E., Matese, J. C., Perou, C. M., Hurt, M. M., Brown, P. O., and Botstein, D. (2002) *Mol. Biol. Cell* **13,** 1977–2000
6. Chaudhry, M. A., Chodosh, L. A., McKenna, W. G., and Muschel, R. J. (2002) *Oncogene* **21,** 1934–1942
7. Shedden, K., and Cooper, S. (2002) *Proc. Natl. Acad. Sci. U. S. A.* **99,** 4379–4384
8. Pines, J., and Hunter, T. (1989) *Cell* **58,** 833–846
9. Golsteyn, R. M., Schultz, S. J., Bartek, J., Ziemiecki, A., Ried, T., and Nigg, E. A. (1994) *J. Cell Sci.* **107,** 1509–1517
10. Ayad, N. G., Rankin, S., Murakami, M., Jebanathirajah, J., Gygi, S., and Kirschner, M. W. (2003) *Cell* **113,** 101–113
11. Zhou, H., Kuang, J., Zhong, L., Kuo, W. L., Gray, J. W., Sahin, A., Brinkley, B. R., and Sen, S. (1998) *Nat. Genet.* **20,** 189–193
12. Banerjee, S., Brooks, W. S., and Crawford, D. F. (2007) *Oncogene* **26,** 6509–6517
13. Figueroa, J., Saffrich, R., Ansorge, W., and Valdivia, M. (1998) *Chromosoma* (*Berl.*) **107,** 397–405
14. Nabetani, A., Koujin, T., Tsutsumi, C., Haraguchi, T., and Hiraoka, Y. (2001) *Chromosoma* (*Berl.*) **110,** 322–334
15. Fang, G., Yu, H., and Kirschner, M. W. (1998) *Mol. Cell* **2,** 163–171
16. Kallio, M., Weinstein, J., Daum, J. R., Burke, D. J., and Gorbsky, G. J. (1998) *J. Cell Biol.* **141,** 1393–1406
17. Jung, C. R., Hwang, K. S., Yoo, J., Cho, W. K., Kim, J. M., Kim, W. H., and Im, D. S. (2006) *Nat. Med.* **12,** 809–816
18. Liu, Z., Diaz, L. A., Haas, A. L., and Giudice, G. J. (1992) *J. Biol. Chem.* **267,** 15829–15835
19. Brooks, W. S., Banerjee, S., and Crawford, D. F. (2006) *Exp. Cell Res.* **313,** 665–676
20. Freemont, P. S. (2000) *Curr. Biol.* **10,** R84–87
21. Lu, Z., Xu, S., Joazeiro, C., Cobb, M. H., and Hunter, T. (2002) *Mol. Cell* **9,** 945–956
22. Dul, B. E., and Walworth, N. C. (2007) *J. Biol. Chem.* **282,** 18397–18406
23. Goto, E., Ishido, S., Sato, Y., Ohgimoto, S., Ohgimoto, K., Nagano-Fujii, M., and Hotta, H. (2003) *J. Biol. Chem.* **278,** 14657–14668
24. Uchida, D., Hatakeyama, S., Matsushima, A., Han, H., Ishido, S., Hotta, H., Kudoh, J., Shimizu, N., Doucas, V., Nakayama, K. I., Kuroda, N., and Matsumoto, M. (2004) *J. Exp. Med.* **199,** 167–172
25. Coscoy, L., Sanchez, D. J., and Ganem, D. (2001) *J. Cell Biol.* **155,** 1265–1273
26. Aravind, L., Iyer, L. M., and Koonin, E. V. (2003) *Cell Cycle* **2,** 123–126
27. Scheel, H., and Hofmann, K. (2003) *Trends Cell Biol.* **13,** 285–287, 287–288
28. Sherr, C. J., and Roberts, J. M. (2004) *Genes Dev.* **18,** 2699–2711
29. Lee, H., Lee, D. J., Oh, S. P., Park, H. D., Nam, H. H., Kim, J. M., and Lim,

D. S. (2006) *Mol. Cell. Biol.* **26,** 5373–5381
30. Li, T., Inoue, A., Lahti, J. M., and Kidd, V. J. (2004) *Mol. Cell. Biol.* **24,** 3188–3197
31. Brandeis, M., Rosewell, I., Carrington, M., Crompton, T., Jacobs, M. A., Kirk, J., Gannon, J., and Hunt, T. (1998) *Proc. Natl. Acad. Sci. U. S. A.* **95,** 4344–4349
32. Murphy, M., Stinnakre, M. G., Senamaud-Beaufort, C., Winston, N. J., Sweeney, C., Kubelka, M., Carrington, M., Brechot, C., and Sobczak-Thepot, J. (1997) *Nat. Genet.* **15,** 83–86
33. Lavin, M. F., and Shiloh, Y. (1997) *Annu. Rev. Immunol.* **15,** 177–202
34. Tischkowitz, M. D., and Hodgson, S. V. (2003) *J. Med. Genet.* **40,** 1–10
35. Elson, A., Wang, Y., Daugherty, C. J., Morton, C. C., Zhou, F., Campos-Torres, J., and Leder, P. (1996) *Proc. Natl. Acad. Sci. U. S. A.* **93,** 13084–13089
36. D'Andrea, A. D. (2003) *Genes Dev.* **17,** 1933–1936
37. Liu, Q., Guntuku, S., Cui, X. S., Matsuoka, S., Cortez, D., Tamai, K., Luo, G., Carattini-Rivera, S., DeMayo, F., Bradley, A., Donehower, L. A., and Elledge, S. J. (2000) *Genes Dev.* **14,** 1448–1459
38. Brown, E. J., and Baltimore, D. (2000) *Genes Dev.* **14,** 397–402
39. Liu, C. Y., Flesken-Nikitin, A., Li, S., Zeng, Y., and Lee, W. H. (1996) *Genes Dev.* **10,** 1835–1843
40. Ludwig, T., Chapman, D. L., Papaioannou, V. E., and Efstratiadis, A. (1997) *Genes Dev.* **11,** 1226–1241
41. Sharan, S. K., Morimatsu, M., Albrecht, U., Lim, D. S., Regel, E., Dinh, C., Sands, A., Eichele, G., Hasty, P., and Bradley, A. (1997) *Nature* **386,** 804–810
42. Suzuki, A., de la Pompa, J. L., Hakem, R., Elia, A., Yoshida, R., Mo, R., Nishina, H., Chuang, T., Wakeham, A., Itie, A., Koo, W., Billia, P., Ho, A., Fukumoto, M., Hui, C. C., and Mak, T. W. (1997) *Genes Dev.* **11,** 1242–1252
43. Wei, J., Zhai, L., Xu, J., and Wang, H. (2006) *J. Biol. Chem.* **281,** 22537–22544
44. Huibregtse, J. M., Scheffner, M., Beaudenon, S., and Howley, P. M. (1995) *Proc. Natl. Acad. Sci. U. S. A.* **92,** 2563–2567
45. Kang, D., Chen, J., Wong, J., and Fang, G. (2002) *J. Cell Biol.* **156,** 249–259
46. Weissman, A. M. (2001) *Nat. Rev. Mol. Cell. Biol.* **2,** 169–178
47. Honda, Y., Tojo, M., Matsuzaki, K., Anan, T., Matsumoto, M., Ando, M., Saya, H., and Nakao, M. (2002) *J. Biol. Chem.* **277,** 3599–3605
48. Salvat, C., Wang, G., Dastur, A., Lyon, N., and Huibregtse, J. M. (2004) *J. Biol. Chem.* **279,** 18935–18943
49. Huang, L., Kinnucan, E., Wang, G., Beaudenon, S., Howley, P. M., Huibregtse, J. M., and Pavletich, N. P. (1999) *Science* **286,** 1321–1326
50. Aravind, L., and Koonin, E. V. (2000) *Curr. Biol.* **10,** R132–R134
51. Swanson, R., Locher, M., and Hochstrasser, M. (2001) *Genes Dev.* **15,** 2660–2674
52. Coscoy, L., and Ganem, D. (2003) *Trends Cell Biol.* **13,** 7–12
53. Allen, R. T., Hunter, W. J., 3rd, and Agrawal, D. K. (1997) *J. Pharmacol. Toxicol. Methods* **37,** 215–228
54. Shi, W., Stampas, A., Zapata, C., and Baker, N. E. (2003) *Genetics* **165,** 1869–1879
55. Ciemerych, M. A., Kenney, A. M., Sicinska, E., Kalaszczynska, I., Bronson, R. T., Rowitch, D. H., Gardner, H., and Sicinski, P. (2002) *Genes Dev.* **16,** 3277–3289
56. Kozar, K., Ciemerych, M. A., Rebel, V. I., Shigematsu, H., Zagozdzon, A., Sicinska, E., Geng, Y., Yu, Q., Bhattacharya, S., Bronson, R. T., Akashi, K., and Sicinski, P. (2004) *Cell* **118,** 477–491
57. Xiao, J., Xu, M., Li, J., Chang Chan, H., Lin, M., Zhu, H., Zhang, W., Zhou, Z., Zhao, B., and Sha, J. (2002) *Biochem. Biophys. Res. Commun.* **291,** 101–110
58. Saunders, D. N., Hird, S. L., Withington, S. L., Dunwoodie, S. L., Henderson, M. J., Biben, C., Sutherland, R. L., Ormandy, C. J., and Watts, C. K. (2004) *Mol. Cell. Biol.* **24,** 7225–7234